Contents lists available at YXpublications

International Journal of Applied Mathematics in Control Engineering

Journal homepage: http://www.ijamce.com

# Rapid Control Strategy of Ballistic Correction Projectile for Small-Caliber Anti-Aircraft Guns Based on UKF Parameter Estimation Algorithm

Shijun Duan[a], Liangming Wang[a], Jian Fu[a,*]

[a] School of Energy and Power Engineering, Nanjing University of Sciences and Technology, Nanjing, 210094, CHN

ARTICLE INFO

Article history:
Received 2 February 2022
Accepted 7 April 2022
Available online 10 April 2022

Keywords:
Anti-aircraft trajectory correction
Impulse control
Two-point boundary value problem
Unscented Kalman filter
Parameter estimation

ABSTRACT

The trajectory correction problem of anti-aircraft gun ammunition based on lateral impulse force can be described as a kind of two-point boundary value problem of nonlinear system. A new method for controlling the projectile-borne actuator is proposed to address the problems of the traditional solution method which is computationally intensive and sensitive to the initial value. In this paper, a pulse force action angle optimization method based on unscented Kalman filter (UKF) parameter estimation algorithm is proposed to solve the two-point boundary value problem. The optimal pulse engine action angle is combined with the relationship model between the total trajectory correction and ignition time and the number of working stages of the pulse engine obtained by regression analysis, and the control method of actuator is obtained. The effectiveness of the method is verified by a simulation example.



## 1. Introduction

Small-caliber anti-aircraft guns, the mainstay of land-based close-range terminal air defense weapons, assume the important tasks of air defense security and air cover, are mainly used to deal with air targets such as helicopters, drones, and precision-guided munitions (e.g., Zhang et al., 2020). In order to improve the striking capability of small-caliber anti-aircraft guns against mobile targets, small pulse engines are used as actuators in ballistic correction technology because of their fast response time (e.g., Wang et al., 2021). The direct lateral force generated by the pulse engine and the aerodynamic force caused by the pulse action are used to change the velocity deflection angle of the projectile to achieve the purpose of ballistic correction (e.g., Yang et al., 2021).

The control parameters of the pulse engine as the actuator of the small-caliber anti-aircraft gun correction projectile include the ignition angle, the ignition moment and the number of pulse operating stages, which work together to determine the ballistic correction effect. The literature (e.g., Zheng et al., 2008) verifies the flight stability and ballistic correction capability of small-caliber anti-aircraft ammunition under the action of pulse force by numerical simulation, but the specific calculation method of the control parameters was not given. The ballistic correction problem of anti-aircraft ammunition based on impulse force is often described as a two-point boundary value problem of nonlinear system, and the analytical solution is very complex and difficult to be solved because of its nonlinearity and abrupt state changes. Therefore, numerical methods are often used to solve the problem (e.g., Betts, 1998). The literature (e.g., Yao, 2021) uses the shooting method which belongs to the numerical solution to calculate the ignition angle of the impulse engine, but it cannot avoid the problem that the calculation result is sensitive to the initial value and prone to local convergence. Leif Walter studies the interception guidance problem of impulse missile and pointed out that the main obstacle of the numerical solution of the two-point boundary value problem is the computational speed, and the computational efficiency is improved by optimizing the control model, but the solution is still performed by using the traditional multiple shooting method (e.g., Walter et al., 2021). Some scholars regard the two-point boundary value problem as a dynamic programming problem and use intelligent optimization algorithms such as particle swarm to find the optimal solution for the control parameters (e.g., Yang et al., 2011; e.g., Li et al., 2016; e.g., Zeehan et al., 2010), but there is a general disadvantage of computationally intensive solution time (e.g., Venter et al., 2002; e.g., Liu et al., 2018).

The unscented Kalman filter（UKF) algorithm is based on the

* Corresponding author.
E-mail addresses: fujian@njust.edu.cn (J. Fu)

estimation theory (e.g., Zhang et al., 2019), which can avoid the problem that the traditional numerical solution of two-point boundary value problem is sensitive to the initial value and difficult to converge. The basic idea is to randomize the original system, assume that the system state variables all satisfy the Gaussian distribution, and convert the original two-point boundary value problem into an optimal parameter estimation problem (e.g., Li et al., 2014; e.g., Zang et al., 2021). The UKF algorithm can be used to recursively correct the beginning state of the system until the filtering converges, so as to obtain the solution of the original two-point boundary value problem.

In view of the advantages of UKF algorithm in solving two-point boundary value problems and the problems of current small-caliber pulse correction anti-aircraft ammunition control methods, this paper proposes a fast control strategy for small-caliber anti-aircraft ammunition correction ammunition based on UKF parameter estimation algorithm. The optimal control model of projectile motion is established for the pulse force action angle, and the pulse force action angle is solved by the UKF parameter estimation algorithm, based on which the pulse ignition moment and the number of working stages are calculated by using the regression model to obtain the pulse engine control strategy for small-caliber anti-aircraft ammunition. The idea of solving the pulse force action angle separately from the pulse engine ignition moment and the number of working stages reduces the computational effort and greatly improves the efficiency of solving the actuator control commands.

## 2. Solving the Pulse Force Action Angle by UKF Parameter Estimation

### *2.1 Projectile Motion Model Based on Direct Lateral Force*

The pulse control method can be divided into direct force control which the pulse force acts at the center of mass and torque control which does not act at the center of mass. For the fin-stabilized projectile as shown in Figure. 1, by placing the pulse engine in front of the projectile center of mass, the direct force of the pulse and the aerodynamic effect caused by the pulse can be superimposed to produce a greater correction effect. As the direct force action of pulse and aerodynamic action caused by pulse can produce the same velocity correction direction, so it is possible to simplify the model by using a projectile motion model based on direct force instead of the full 6-degree-of-freedom torque control projectile motion model to characterize the effect of the pulse force action angle on the ballistic correction direction, thus increasing the computational speed.

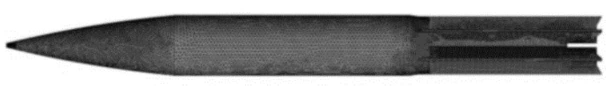

**Fig.1.** Small-caliber Anti-aircraft ballistic correction projectile

Due to the rotation of the projectile, the pulse engine turns through a sector during operation, as shown in Figure 2.

$\gamma_1$ is the pulse force action angle, then the pulse engine ignition angle is expressed as:

$$\gamma_p = \gamma_1 - \omega\tau / 2 \tag{1}$$

where $\omega$ is the angular velocity of projectile roll and $\tau$ is the individual pulse engine working duration.

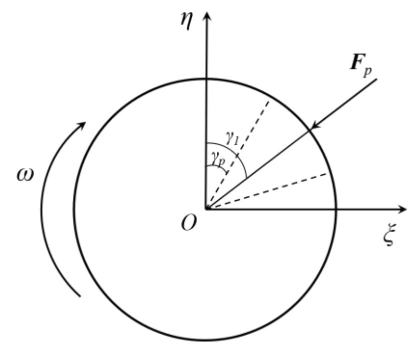


**Fig.2.** Schematic diagram of the action of the pulse force

The following model of projectile motion based on direct lateral force is developed.
Status variables:

$$X = [v\ \theta\ \psi_1\ \psi_2\ x\ y\ z]^{\mathrm{T}} \tag{2}$$

Control variables:

$$u(t) = \gamma_1 \tag{3}$$

State equation:

$$\dot{X}(t) = f[X(t), u(t), t] \tag{4}$$

$$\begin{cases} \dot{v} = -\dfrac{1}{2m}\rho(y)sc_x v^2 - g\sin(\theta+\psi_1) \\ \dot{\theta} = -g\cos\theta / v \\ \dot{\psi}_1 = g\sin\theta\sin\psi_1 / v - \dfrac{P\cos\gamma_1}{mv} \\ \dot{\psi}_2 = g\sin\theta\sin\psi_2 / v - \dfrac{P\sin\gamma_1}{mv} \\ \dot{x} = v\cos\psi_2\cos(\theta+\psi_1) \\ \dot{y} = v\cos\psi_2\sin(\theta+\psi_1) \\ \dot{z} = v\sin\psi_2 \end{cases} \tag{5}$$

where $m$ is the projectile mass, $v$ is the projectile velocity, $\theta$ is the ballistic inclination, $\psi_1$ and $\psi_2$ are the high and low ballistic deflection angles and lateral ballistic deflection angles, $x, y, z$ is the projectile position coordinates in space, $\gamma_1$ is the angle between the nozzle of the pulse engine and the axis $O\eta$ in the first projectile axis coordinate system $O\xi\eta\zeta$, $P$ is the impulse of the pulse engine, $\rho(y)$ is the air density at the altitude of the projectile, $s$ is the cross-sectional area of the projectile, $c_x$ is the drag coefficient, and $g$ is the acceleration of gravity.

The purpose of performing ballistic correction is to correct the deviation of the drop point due to various uncertainties, which requires the projectile to move from the current state $X(t_0)$ to the desired state $X(t_f)$ in the shortest possible time, so the performance index is taken as:

$$\min_{\boldsymbol{u}(t)} J = \int_{t_0}^{t_f} L(\boldsymbol{x}, \boldsymbol{u}, t)\mathrm{d}t = \int_{t_0}^{t_f} \mathrm{d}t = t_f - t_0 \tag{6}$$

which is an integral type performance indicator with free $t_f$ and fixed end. To solve the optimal pulse force action angle $\gamma_1$, the Hamiltonian function is introduced by the state equation:

$$
\begin{aligned}
&H(\boldsymbol{x},\boldsymbol{u},\boldsymbol{\lambda},t)=L(\boldsymbol{x},\boldsymbol{u},t)+\boldsymbol{\lambda}^{\mathrm{T}}f(\boldsymbol{x},\boldsymbol{u},t)\\
&=1+\lambda_v(-\frac{1}{2m}\rho(y)sc_x v^2-g\sin(\theta+\psi_1))-\lambda_\theta g\cos\theta/v\\
&+\lambda_{\psi1}(g\sin\theta\sin\psi_1/v-\frac{P\cos\gamma_1}{mv})\\
&+\lambda_{\psi2}(g\sin\theta\sin\psi_2/v-\frac{P\sin\gamma_1}{mv})\\
&+\lambda_x v\cos\psi_2\cos(\theta+\psi_1)+\lambda_y v\cos\psi_2\sin(\theta+\psi_1)+\lambda_z v\cos\psi_2
\end{aligned}
\tag{7}
$$

where $\lambda_v$, $\lambda_\theta$, $\lambda_{\psi1}$, $\lambda_{\psi2}$, $\lambda_x$, $\lambda_y$, $\lambda_z$ are the Lagrange multipliers corresponding to the state variables. According to the optimization theory, to follow the optimal flight trajectories $X(t)$ and $\lambda(t)$ , the following regular equations should be satisfied:
State equation:

$$\dot{X}(t)=-\frac{\partial H}{\partial\lambda}=f[X(t),u(t),t] \tag{8}$$

Costate equation:

$$\dot{\lambda}(t)=-\frac{\partial H}{\partial X} \tag{9}$$

Due to control of unconstrained, extreme value condition:

$$\frac{\partial H}{\partial\gamma_1}=\frac{\lambda_{\psi1}P\sin\gamma_1}{mv}-\frac{\lambda_{\psi2}P\sin\gamma_1}{mv}=0 \tag{10}$$

$$\gamma_1=\arctan\frac{\lambda_{\psi2}}{\lambda_{\psi1}} \tag{11}$$

The value range of $\gamma_1$ is [0, 360] deg.
Initial boundary conditions:

$$
\begin{aligned}
X(t_0)&=[v(t_0)\ \ \theta(t_0)\ \ \psi_1(t_0)\ \ \psi_2(t_0)\ \ x(t_0)\ \ y(t_0)\ \ z(t_0)]^{\mathrm{T}}\\
&=[v_0\ \ \theta_0\ \ \psi_{10}\ \ \psi_{20}\ \ x_0\ \ y_0\ \ z_0]^{\mathrm{T}}
\end{aligned}
\tag{12}
$$

Terminal boundary conditions:

$$
\begin{aligned}
X(t_f)&=[v(t_f)\ \ \theta(t_f)\ \ \psi_1(t_f)\ \ \psi_2(t_f)\ \ x(t_f)\ \ y(t_f)\ \ z(t_f)]^{\mathrm{T}}\\
&=[v_f\ \ \theta_f\ \ \psi_{1f}\ \ \psi_{2f}\ \ x_f\ \ y_f\ \ z_f]^{\mathrm{T}}
\end{aligned}
\tag{13}
$$

The system of differential equations consisting of the state equation (8) and the costate equation (9) is a typical two-point boundary value problem. The initial moment $t_0$ and the initial states $v_0$, $\theta_0$, $\psi_{10}$, $\psi_{20}$, $x_0$, $y_0$, $z_0$ are known, the terminal moment $t_f$ and the terminal states $x_0$, $y_0$, $z_0$ are known, and the other state variables $v_t$, $\theta_t$, $\psi_{1t}$, $\psi_{2t}$ are free and unconstrained. The optimal control variable can minimize the deviation of the projectile from the target.

### 2.2 UKF Parameter Estimation Algorithm

This section discusses how the above two-point boundary value problem can be rewritten as a parameter estimation problem and solved using the UKF estimation method. The initial values of the costate variables $\lambda_{\psi1}(t_0)$ and $\lambda_{\psi2}(t_0)$ related to the pulse force action angle are selected as the parameters to be estimated. Let the range $x$ at which the projectile reaches the target be the integration stop condition, so that the terminal constraints are $y(t_f)$ and $z(t_f)$. The estimated parameters $\boldsymbol{w}_k$ and the desired output $\boldsymbol{d}_k$ are:

$$\boldsymbol{w}_k=[\lambda_{\psi1}(t_0),\lambda_{\psi2}(t_0)]^{\mathrm{T}} \tag{14}$$

$$\boldsymbol{d}_k=[y(t_f),z(t_f)]^{\mathrm{T}} \tag{15}$$

The purpose of the parameter estimation problem is to determine the following nonlinear mapping:

$$y_k=G(x_k,\ w),\ \ k=1,\ 2,\ \cdots,\ \infty, \tag{16}$$

where $(x_k, y_k)$ is the known sequence of mapping pairs, $x_k$ is the input, and $y_k$ is the output; $w$ is the unknown estimated parameters.

Define the output error $e_k=d_k-G(x_k,\ w)$ , where $d_k$ is the desired output. Solving the parameter estimation problem is to estimate the mean of $w$ so that the output error of the mapping $G(x_k,\ w)$ is minimized.

The nonlinear mapping (16) is transformed as follows and written in the form of a state space expression:

$$
\begin{aligned}
w_{k+1}&=w_k+r_k\\
d_k&=G(x_k,\ w)+e_k
\end{aligned}
\tag{17}
$$

where $w_k$ is a stationary stochastic process with a unitary array of state transfer matrix, the expected output $d_k$ corresponds to a nonlinear observation of the estimated parameter $w_k$ , the system noise $r_k$ and the observation noise $e_k$ are both Gaussian white noise. Then, the original parameter estimation problem can be solved by using various Kalman filters to give the minimum variance estimate $\hat{w}_k$ of the unknown parameter $w_k$ as the solution of Eq.(16).

The parameter estimation process based on the UKF is as follows:

(1) Initialization

$$
\begin{aligned}
\hat{w}_0&=E(w),\\
P_{w0}&=E((w-\hat{w}_0)(w-\hat{w}_0)^{\mathrm{T}})
\end{aligned}
\tag{18}
$$

(2) State update and $\sigma$ -points calculation

$$\hat{w}_{k|k-1}=\hat{w}_{k-1}, \tag{19}$$

$$
\begin{aligned}
R_k^{\ r}&=(\rho^{-1}{}_{\mathrm{RLS}}-1)P_{w_k},\\
P_{k|k-1}&=P_{k-1}+R^r{}_{k-1},\\
W_{k|k\text{-}1}&=(\hat{w}_{k|k\text{-}1},\hat{w}_{k|k\text{-}1}+\gamma\sqrt{P_{k|k\text{-}1}},\hat{w}_{k|k\text{-}1}-\gamma\sqrt{P_{k|k\text{-}1}}),\\
D_{k|k-1}&=G(x_k,W_{k|k-1}),\\
\hat{d}_k&=\sum_{i=0}^{2L}W_i^{(m)}D_{i,k|k-1}.
\end{aligned}
\tag{20}
$$

(3) Observation update

$$
\begin{aligned}
P_{d_k d_k}&=\sum_{i=0}^{2N}W_i^{(c)}[D_{i,k|k-1}-\hat{d}_k][D_{i,k|k-1}-\hat{d}_k]^{\mathrm{T}}+R_k^e,\\
P_{w_k d_k}&=\sum_{i=0}^{2N}W_i^{(c)}[W_{i,k|k-1}-\hat{w}_k][D_{i,k|k-1}-\hat{d}_k]^{\mathrm{T}},\\
K_k&=P_{w_k d_k}P_{w_k d_k}^{-1},\\
\hat{w}_k&=\hat{w}_{k|k-1}+K_k(d_k-\hat{d}_k),\\
P_{w_k}&=P_{w_k}^{-1}-K_k P_{d_k d_k}K_k^{\mathrm{T}}.
\end{aligned}
\tag{21}
$$

In the above algorithm formula:

$$
\begin{cases}
\alpha=\sqrt{N+\eta}\\
\eta=\varepsilon^2(N+\kappa)-N\\
W_0^{(m)}=\eta/(N+\eta)\\
W_0^{(c)}=\eta/(N+\eta)+(1-\varepsilon^2+\beta)\\
W_i^{(m)}=W_i^{(c)}=0.5/(N+\eta)\quad i=1,2,\cdots,2N
\end{cases}
\tag{22}
$$

where $N$ is the dimensionality of the estimated parameter $w$ , $\eta$

is the scaling parameter, which is used to reduce the overall prediction error, and $\varepsilon$ determines the distribution range of $\sigma$ -points relative to the current $w$ mean value at the time of UT transformation, which generally takes the value range of $[10^{-4},1]$. The constant $\kappa$ takes the value of $3-N$ or 0. $\beta$ is a constant associated with the $w$ prior distribution and takes the value of 2 which is optimal for Gaussian distribution. $\rho_{\mathrm{RLS}}$ is the forgetting factor, which is used to prevent the filtering divergence caused by the model error, takes the value range of $(0,1]$ and can be set to gradually increase with the filtering process.

The above UKF parameter estimation algorithm is used to solve the two-point boundary value problem of the optimal control model, and the following example is given to solve the optimal pulse force action angle, the specific values of the parameters in the example are shown in Table 1. It is assumed that an impulse is applied at the starting moment to correct the ballistic, based on which the pulse force action angle is optimized and minimizes the deviation of the projectile from the target by the UKF parameter estimation algorithm.

Tab.1. Simulation parameters

| parameters | value | parameters | value |
|---|---|---|---|
| $m$/(kg) | 0.609 | $\psi_{20}$ /(° ) | 0 |
| $S$/(m2) | 0.000962 | $x_0$ /(m) | 0 |
| $P$/(N) | 500 | $y_0$ /(m) | 0 |
| $Cx$ | 0.2902 | $z_0$ /(m) | 0 |
| $V_0$ /(m/s) | 950 | $x_f$ /(m) | 1300 |
| $\theta_0$ /(deg) | 45 | $y_f$ /(m) | 1330 |
| $\psi_{10}$ /(deg) | 0 | $z_f$ /(m) | -20 |

Set the initial value of estimation parameter $\boldsymbol{w}_0=[1.1,\ 0.1]^{\mathrm{T}}$, and get the change curve of the deviation of the projectile from the target with the execution process of UKF parameter estimation algorithm as Figure 3, and the corresponding change curve of estimation parameter as Figure 4.

In this example, the minimum deviation of the projectile from the target is obtained when the UKF parameter estimation algorithm is executed to the 6th step, at this time the estimated parameter is $\boldsymbol{w}_k=[1.1244,\ -0.5510]^{\mathrm{T}}$. From the Eq.(11), the pulse force action angle is 153.89deg or 333.89deg, combined with the specific correction direction, the optimal pulse force action angle is determined to be 153.89deg.

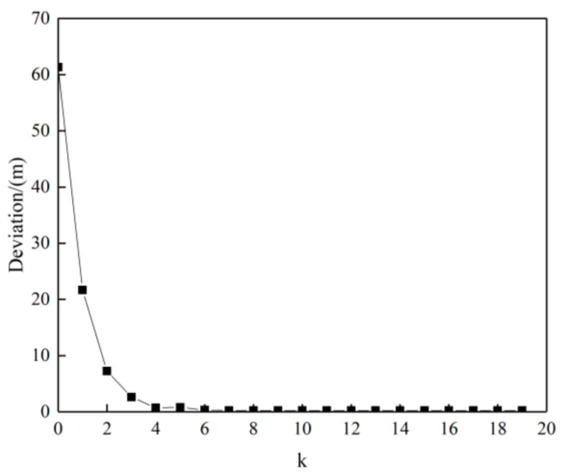


**Fig.3.** Variation curve of the deviation of the projectile from the targe

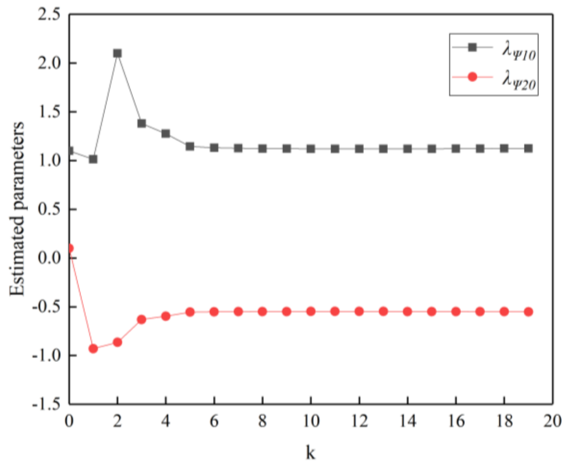


**Fig.4.** Estimated parameter variation curves

## 3. Model of the Relationship between the Actuator Control Parameters and the Ballistic Correction Quantity

In the case of known firing data, the ballistic correction process of impulse-corrected small-caliber anti-aircraft projectiles can be regarded as a multiple-input and multiple-output control system, where the input is the control parameters of the actuator, i.e., the ignition angle, the ignition moment and the number of working stages of the pulse engine, and the output is the corrected bullet impact point. In order to avoid complex differential equation calculation, this control system can be regarded as a black box, and the empirical equations of input and output parameters can be summarized through finite ballistic simulation tests (e.g., Zhao et al., 2019). Based on this idea, this section uses uniform design to arrange ballistic simulation tests to study the relationship between the actuator control parameters and ballistic correction quantity of impulse-corrected small-caliber anti-aircraft projectiles.

The coordinate of target $M_f$ in space is $(x_f, y_f, z_f)$. The coordinate of the impact point of the projectile when it reaches the range $x_f$ where the target is located without the action of the actuator is $(x_f, y_m, z_m)$. The required ballistic correction quantity is defined as follows:

$$\Delta L=\sqrt{(y_f-y_m)^2+(z_f-z_m)^2} \tag{23}$$

It has been shown that under the same firing data conditions, when the pulse engine ignition moment and the number of working stages are the same, different pulse action angles have no effect on the total ballistic correction quantity, so the controllable factors of the experimental design are: factor 1(X1) is the shot angle $\theta_0$, taking the value range of 10~79deg; factor 2(X2) is the number of pulse engine working stages $n$, taking the value range of 1~8; factor 3(X3) is the pulse engine ignition moment $t_p$, the value range is 1.0~3.0s; factor 4(X4) is the projectile flight time, the value range is 1.5~5.0s. Referring to the value range of each factor for the selection of the level number, the level numbers of the four factors are taken as 24, 8, 6 and 6, the level numbers among the factors are different, which belongs to the mixed design, the $U_{24}(24^1 8^1 6^2)$ table used in the test is given in Table 2.

**Tab.2**. $U_{24}(24^1 8^1 6^2)$ uniform design table

| Number of tests | U24 | | | | Number of tests | U24 | | | |
|---|---|---|---|---|---|---|---|---|---|
| | X1 | X2 | X3 | X4 | | X1 | X2 | X3 | X4 |
| 1 | 1 | 2 | 3 | 4 | 13 | 13 | 1 | 5 | 2 |
| 2 | 2 | 4 | 6 | 2 | 14 | 14 | 3 | 1 | 6 |
| 3 | 3 | 6 | 2 | 6 | 15 | 15 | 5 | 4 | 4 |
| 4 | 4 | 8 | 5 | 4 | 16 | 16 | 7 | 1 | 2 |
| 5 | 5 | 2 | 2 | 2 | 17 | 17 | 1 | 3 | 6 |
| 6 | 6 | 4 | 4 | 6 | 18 | 18 | 3 | 6 | 4 |
| 7 | 7 | 6 | 1 | 3 | 19 | 19 | 5 | 3 | 1 |
| 8 | 8 | 8 | 4 | 1 | 20 | 20 | 7 | 5 | 5 |
| 9 | 9 | 2 | 6 | 5 | 21 | 21 | 1 | 2 | 3 |
| 10 | 10 | 4 | 3 | 3 | 22 | 22 | 3 | 5 | 1 |
| 11 | 11 | 6 | 6 | 1 | 23 | 23 | 5 | 1 | 5 |
| 12 | 12 | 8 | 2 | 5 | 24 | 24 | 7 | 4 | 3 |

The following quadratic regression model was chosen to characterize the relationship between the actuator control parameters and the ballistic correction quantity for the impulse-corrected small-caliber anti-aircraft projectile:

$$Y = b + \sum_{i=1}^{M} a_i X_i + \sum_{i=1}^{M} a_{ii} X_i^2 + \sum_{i<j} a_{ij} X_i X_j \tag{24}$$

where $Y$ is the test index, $X_1 \sim X_4$ are the four factors, $a$ and $b$ are the regression coefficients, and $M = 4$.

Stepwise regression analysis is used to filter the variables, analyze and process the simulation data to finally obtain the following regression model:

$$Y = 0.3324 + 1.9142X_2 - 3.6107X_2X_3 + 3.1046X_2X_4 \tag{25}$$

The analysis shows that the adjusted $R^2$ of this regression model is 0.998, the significance less than 0.001, and the model statistic $F = 2873.276$. It indicates that the model fits well, there is a significant correlation between the independent variables and dependent variables, and the regression equation (25) is very significant, which can accurately represent the relationship between the actuator control parameters and the ballistic correction quantity.

## 4. Actuator Control Method for Impulse-Corrected Small- Caliber Anti-Aircraft Projectile

According to the theory of anti-aircraft gun fire, the flight time of the projectile $t_f$ is given by the prediction of the fire control system, while the predicted value of the deviation of the projectile from the target, i.e., the required ballistic correction quantity $\Delta L$, can be obtained in combination with the regression model of the ballistic correction Eq.(25), the starting ignition moment of the impulse engine of the impulse-corrected small-caliber anti-aircraft projectile can be obtained as follows:

$$t_p = \frac{\Delta L - 0.3324 - 1.9142n - 3.1046nt_f}{3.6107n} \tag{26}$$

where $t_p$ is the ignition moment of the pulse engine, $n$ is the number of pulse engine working stages, $t_f$ and $\Delta L$ are the predicted values of projectile flight time and the deviation of the projectile from the target given by the fire control system. Due to the limitation of the data processing speed of the artillery fire control system and the structure of the artillery ammunition itself, the value of the actuator control parameter combination $(t_p, n)$ should satisfy $1 < t_p < t_f, 1 \le n \le 8$, and $n$ is an integer.

There may be multiple valid solutions for the combination of control parameters $(t_p, n)$. In order to reduce the impact of pulse engine operation on the range and leave more adequate reaction time for the fire control system, $t_p$ is maximized as a secondary optimization indicator, then the control method of the anti-aircraft artillery pulse correction bullet actuator is as following:

(1) The ground station tracks the motion parameters of the target and the projectile, giving the predicted values of the target future point $M_f(x_f, y_f, z_f)$ and the predicted values of the flight time $t_f$ for the projectile to reach the target range $x_f$ and the impact point $M_0(x_f, y_m, z_m)$.

(2) Calculate the required ballistic correction quantity $\Delta L$ based on the future point of the target and the point of impact, and compare it to the destruction radius of the projectile to determine if ballistic correction is required.

(3) If ballistic correction is required, the projectile flight time $t_f$ and the required ballistic correction quantity $\Delta L$ are substituted into Eq.(25), and $n$ is taken as an integer from 1 to 8. All combinations $(t_p, n)$ of control parameters that meet the constraints are calculated, and the set with condition $\max\{t_p\}$ is selected as the desired pulse engine ignition moment and working stages.

(4) Based on the optimal pulse force action angle obtained by the UFK parameter estimation algorithm in Section 2, the pulse engine ignition angle can be derived as:

$$\gamma_p = \gamma_1 - \frac{\omega\tau}{2} \tag{27}$$

where $\omega$ is the current angular velocity of the projectile roll, obtained from the bullet-loaded geomagnetic sensor, and $\tau$ is the pulse engine working time.

This gives the complete impulse-corrected small-caliber anti-aircraft projectile actuator control command $(t_p, n, \gamma_p)$.

## 4.Simulation

The ballistic model simulation is performed based on the above control method, the ballistic model is a full 6-degree-of-freedom rigid body ballistic equation (e.g., Han et al., 2014) and the results are compared with the correction effect of the control command obtained by particle swarm optimization to verify the effectiveness of the proposed method.

**Tab.3**. Simulation test data

| Firing angle | Actual point of impact | | | Target position | | |
|---|---|---|---|---|---|---|
| $\theta$/（°） | x | y | z | x | y | z |
| 20 | 1500 | 525.98 | -0.0083 | 1500 | 500 | 32 |
| 35 | 2050 | 1371.97 | -0.024 | 2050 | 1358 | -20 |
| 50 | 1256.72 | 1465.05 | -0.0095 | 1256.72 | 1465 | -45 |
| 70 | 960 | 2552.36 | -0.0138 | 960 | 2565 | 20 |

**Tab.4**. Trajectory correction result of the proposed method

| Control command | | | Corrected point of impact | | |
|---|---|---|---|---|---|
| $t_p$ | $n$ | $\gamma_p$ | x | y | z |
| 1.0056 | 8 | 308 | 1500 | 499.405 | 31.771 |
| 3.2370 | 8 | 60.53 | 2050 | 1358.06 | -21.0826 |
| 1.4405 | 8 | 89.44 | 1256.72 | 1464.17 | -46.6283 |
| 4.1119 | 8 | 256.75 | 960 | 2564.6 | 20.6003 |

**Tab.5.** Particle swarm optimization algorithm results

| Control command | | | Corrected point of impact | | |
|---|---|---|---|---|---|
| $t_p$ | $n$ | $\gamma_p$ | x | y | z |
| 1.000 | 8 | 307.638 | 1500 | 499.499 | 32.0978 |
| 2.855 | 5 | 59.131 | 2050 | 1357.83 | -19.9929 |
| 1.000 | 6 | 89.846 | 1256.72 | 1464.69 | -45.9575 |
| 1.950 | 2 | 255.283 | 960 | 2562.77 | 20.6581 |

Table 3 shows the known simulation data, including the target point and the spatial coordinates of the actual impact point under different firing angles. Table 4 shows the control commands and the corrected impact point derived from the control method proposed in this paper. The results indicates that the corrected impact point is very close to the target position, and the hitting accuracy of the anti-aircraft gun has been significantly improved.

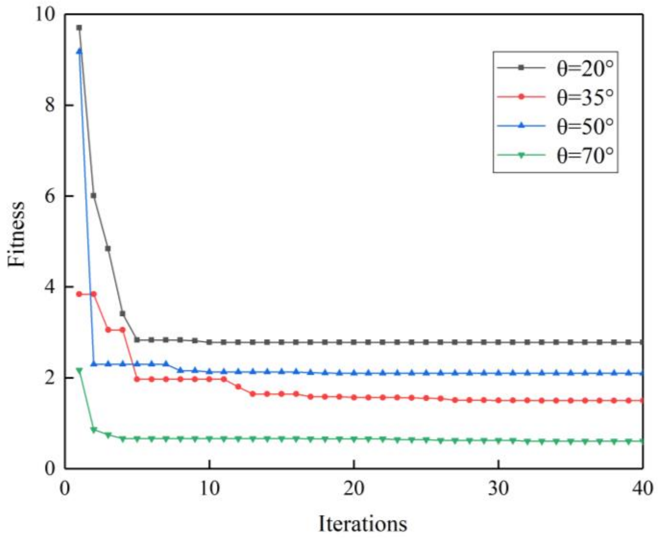


**Fig.5.** Particle swarm algorithm convergence curve

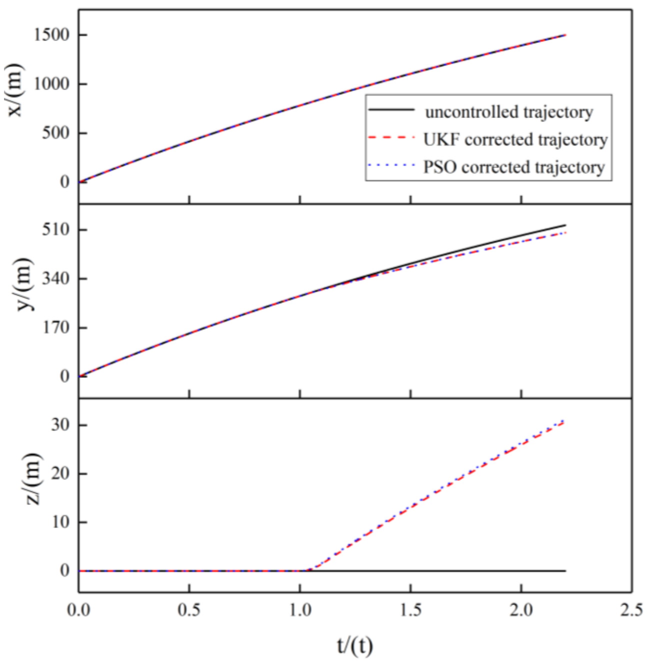


**Fig.6.** Trajectory curve at firing angle of 20 deg

As a comparison, Table 5 shows the control commands obtained by the particle swarm optimization algorithm with a population size of 25 and the corrected impact points. Figure 5 shows the corresponding convergence curves with the fitness function $F=\lambda_1 n+\lambda_2 R$ (e.g., Yang et al., 2011), where $n$ is the number of pulse engine working stages, $R$ is the deviation of the projectile from the target, weighting factors $\lambda_1$、$\lambda_2$ are positive, and $\lambda_1+\lambda_2=1$.

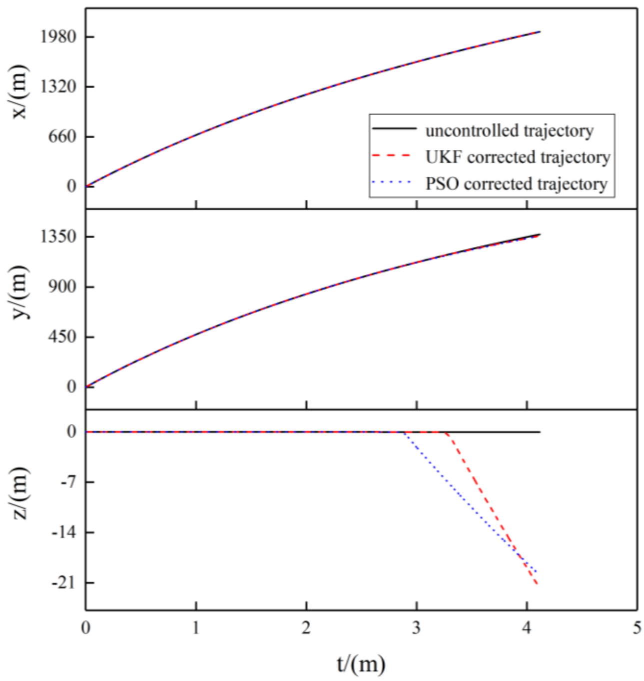


**Fig.7.** Trajectory curve at firing angle of 35 deg

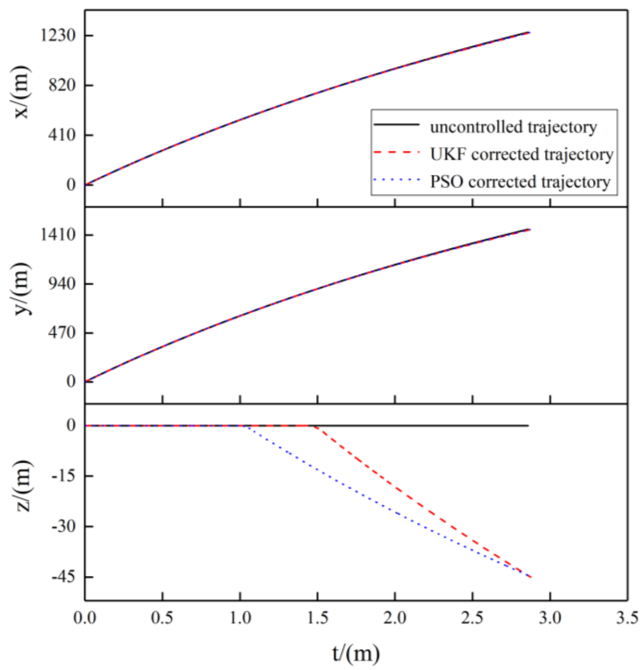


**Fig.8.** Trajectory curve at firing angle of 50 deg

Figures 6 to 9 show the curves of the small-caliber anti-aircraft correction projectile position parameters $x$, $y$, and $z$ obtained through the simulation test data in this section for different firing angles with time. The corrected trajectories obtained by the proposed method and the particle swarm optimization algorithm are compared with the uncontrolled trajectories. Although the actuator control commands derived by the proposed method and the ones obtained by the particle swarm algorithm are slightly different, similar trajectory correction effects are achieved.

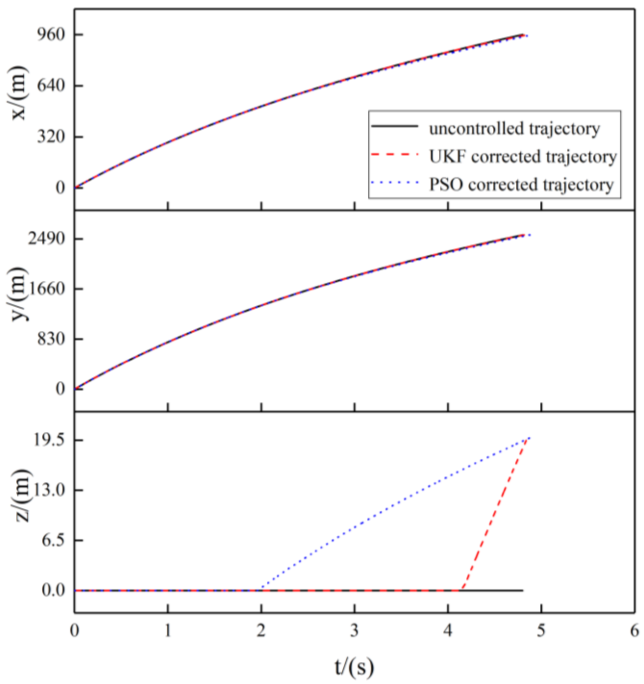


**Fig.9.** Trajectory curve at firing angle of 70 deg

In this example, the particle swarm optimization algorithm requires more than 10 iterations to obtain the available control commands, and because the complete 6-degree-of-freedom ballistic equations are used, the computation time for each iteration step is much longer than that of the UKF parameter estimation algorithm which uses a simplified ballistic model. The average time used to obtain the control command for the particle swarm optimization algorithm is 4920s, while the average time for the control method proposed in this paper is 2.72s, which greatly improves the solution efficiency and is more usable while ensuring the ballistic correction effect.

## 5.Conclusion

In this paper, the trajectory correction of small-caliber anti-aircraft gun projectile with pulse engine as actuator is studied. Aiming at the problem that the traditional calculation method is sensitive to the initial value and has a large amount of calculation, a fast control strategy of the actuator is proposed. The UKF parameter estimation algorithm is used to solve the two-point boundary value problem of a nonlinear system based on the lateral impulse force ballistic correction model for anti-aircraft projectile to obtain the optimal pulse force action angle. The pulse force action angle is combined with the model of the relationship between the actuator control parameters and the ballistic correction quantity obtained by multivariate nonlinear regression to achieve the control commands of the pulse engine. The computational speed is improved under the premise of ensuring the correction accuracy, which provides a new solution for the ballistic correction problem of small-caliber anti-aircraft gun projectiles.

## Acknowledgements

This work was supported by China Postdoctoral Science Foundation under Grant [61603191,61603189], Jiangsu Provincial Natural Science Research Project [20KJD510005]. The authors also gratefully acknowledge the helpful comments and suggestions of the reviewers.

## References

Zhang, C., et al, 2020. Reflections on the Upgrading of the Active Anti-aircraft Gun Weapon System. Journal of Gun Launch & Control. 1-4.

Wang, Z.Y., et al, 2021. Review on Development of Technology of Trajectory Correction Projectile. Journal of Ballistics. 33(2),1-12.

Yang, Z.W., et al, 2022. Motion Characteristics of the Small Caliber Anti-aircraft Gun Correction Projectile Subjected to a Pulse Action. ACTA ARMAMENTARII. 43(6), 1337-1345.

Zheng, Y.S., et al, 2008. Trajectory Correction Technology of Small Caliber Projectile and It' s Simulation Analysis. Journal of Ballistics. 20(1),39-47.

Betts, John. T, 1998. Survey of Numerical Methods for Trajectory Optimization. JOURNAL OF GUIDANCE, CONTROL, AND DYNAMICS. 21,193-207.

Yao, W.J, 2007. Study of Impulse Correction Method for the Two-dimensional Trajectory Correction Anti-aircraft Projectile [Unpublished doctoral dissertation]. Nanjing University of Science and Technology.

Walter, L., et al, 2013. Optimal Control Framework for Impulsive Missile Interception Guidance. AIAA Guidance, Navigation, and Control (GNC) Conference. 1-14.

Yang, H.W., et al, 2011.Reserach on Control Method of Anti-aircraft Correction Ammunition Based on Particle Swarm Optimization. Journal of Ballistics. 23(2), 57-61.

Li, J., et al, 2016. Research on Optimal Method of Impulse Parameters Using Modified Particle Swarm Optimization. Journal of Shenyang Ligong University. 35(4), 62-67.

Zeehan, Q., et al, 2010. Multidisciplinary Design of Multistage Interceptor using Particle Swarm Optimization. 51st AIAA/ASME/ASCE/AHS/ASC Structures, Structural Dynamics, and Materials Conference 18th. 1-7.

Venter, G., et al, 2002. Particle Swarm Optimization. 43rd AIAA/ASME/ASCE/AHS/ASC Structures, Structural Dynamics, and Materials Con, 1-9.

Liu, H., et, al, 2018. The Research Status and Prospect of Particle Swarm Optimization Algorithm for Water Environment Quality Assessment. International Journal of Applied Mathematics in Control Engineering. 1(1), 23-30.

Zhang, H., et, al, 2019. Kalman Federal Filtering Algorithm of UAV Fault-Tolerant Integrated Navigation. International Journal of Applied Mathematics in Control Engineering. 2(1), 100-106.

Li, J., et al, 2014. Unscented Kalman Filter for Low-Thrust Orbit Transfer Optimization. Journal of Astronautics. 35(2), 144-150.

Zang, J., et al, 2021. Application of UKF Filter Algorithm in Solving Two-Point Boundary Value Problem. MODERN DEFENCE TECHNOLOGY.49(4), 35-42.

Zhao, R., et al, 2019. The Identification Method of Missile System Parameter Based on Orthogonal Design. International Journal of Applied Mathematics in Control Engineering. 2(2), 182-187.

Han, Z.P., et al, 2014. Exterior Ballistics of Projectiles and Rockets. BEIJING INSTITUTE OF TECHNOLOGY PRESS.

***Shijun Duan*** is currently pursuing his MS study at School of Energy and Power Engineering, Nanjing University of Sciences and Technology, Nanjing, China. He obtained his BS degree from Nanjing University of Sciences and Technology. His research interest covers control theory of new type of projectiles and rockets.

***Liangming Wang*** is a professor at School of Energy and Power Engineering, Nanjing University of Sciences and Technology. He received the Ph.D. degree in external ballistic engineering from Nanjing University of Sciences and Technology. His research interest covers Aircraft guidance and control technology, dynamic system modeling and algorithm research and so on.

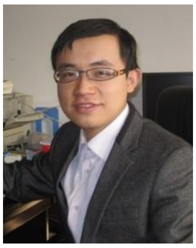

***Jian Fu*** received his Ph.D. degree in control theory and control engineering from Nanjing University of Aeronautics and Astronautics. In the same year, he taught at Nanjing University of Science and Technology. Now, he is an associate researcher at NUST. He mainly engaged in nonlinear control, robust control, sliding mode control, adaptive observer design and so on.